J|A|C|S
ARTICLES
Published on Web 04/19/2006

Computational Study of Carbon Atom (^{3}P and ^{1}D) Reaction with CH_2O. Theoretical Evaluation of $^1B_1$ Methylene Production by C (^{1}D)

Hyun Joo, Philip B. Shevlin, and Michael L. McKee*

Contribution from the Department of Chemistry and Biochemistry, Auburn University, Auburn, Alabama 36849

Received January 11, 2006; E-mail: mckee@chem.auburn.edu

Abstract: Singlet and triplet free energy surfaces for the reactions of C atom (^{3}P and ^{1}D) with CH_2O are studied computationally to evaluate the excited singlet ($^1B_1$) methylene formation from deoxygenation of CH_2O by C (^{1}D) atom as suggested by Shevlin et al. Carbon atoms can react by addition to the oxygen lone pair or to the C═O double bond on both the triplet and singlet surfaces. Triplet C (^{3}P) atoms will deoxygenate to give CO plus CH_2 ($^3B_1$) as the major products, while singlet C (^{1}D) reactions will form ketene and CO plus CH_2 ($^1A_1$). No definitive evidence of the formation of excited singlet ($^1B_1$) methylene was found on the singlet free energy surface. A conical intersection between the $^1A'$ and $^1A''$ surfaces located near an exit channel may play a role in product formation. The suggested $^1B_1$ state of methylene may form via the $^1A''$ surface only if dynamic effects are important. In an effort to interpret experimental observation of products trapped by (*Z*)-2-butene, formation of *cis*- and *trans*-1,2-dimethylcyclopropane is studied computationally. The results suggests that "hot" ketene may react with (*Z*)-2-butene nonstereospecifically.

Introduction

The chemistry of atomic carbon is central to the mechanistic and quantitative understanding of organic chemistry in that it is the ultimate case of a low-valent carbon-centered reactive intermediate that exhibits a thermodynamic drive to form a tetravalent carbon. However, it is very difficult to achieve a complete understanding of C atom reactions because the reaction of C atom produces other reactive intermediates, such as carbenes, which can react to form more stable products. Hence, the experimental studies of the mechanisms of C atom reactions have often been limited, and complementary computational studies have been utilized successfully.[1]

Most reactions of C atoms are highly exothermic because of the extremely high heat of formation of the C atom. The ground-state atomic carbon is triplet (^{3}P), with a heat of formation ($\Delta H_f°$) of 171 kcal/mol. The first and second excited states are singlet states, ^{1}D with $\Delta H_f° = 201$ kcal/mol and ^{1}S with $\Delta H_f° = 233$ kcal/mol, respectively.[1,2] Many of the C atom reactions involve the ^{1}D state, and this species brings an additional 30 kcal/mol of energy to its reaction. Therefore, the products from C atom reactions contain a great deal of excess energy. When the initial product of a C atom reaction is another reactive intermediate such as a carbene, then very interesting reactivity can be observed due to the high exothermicity.[1,3]

When C atoms react with unsaturated hydrocarbons, abstraction of hydrogen, insertion into a C−H bond, or π addition occurs.[1,4−8] In analogy with carbenes,[9] atomic carbon reacts with alkenes by double-bond addition to give cyclopropylidenes which undergo ring-opening to allenes. In the case of carbonyl compounds, the ^{1}D C atom can react in a similar fashion: carbon atom addition to the C═O double bond followed by ring-opening to give a ketene, as shown in eq 1. There is also the

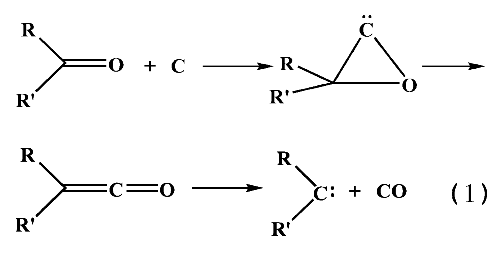

(1)

possibility of end-on attack via a lone pair of electrons on oxygen, forming an ylide-like species ($R_2C{-}O{-}C$). However, no compelling evidence for the end-on intermediate has been reported.[10] Although a ketene is the global minimum on the

(1) Shevlin, P. B. In *Reactive Intermediate Chemistry*; Moss, R. A., Platz, M. S., Jones, M., Jr., Eds.; Wiley: New York, 2004; p 463.
(2) Chase, M. W., Jr. *NIST−JANAF Thermochemical Tables*, 4th ed.; J. Phys. Chem. Ref. Data Monograph 9; American Institute of Physics: Washington, DC, 1998.
(3) (a) Wolf, A. P. *Adv. Phys. Org. Chem.* **1964**, *2*, 201. (b) Wolfgang, R. *Prog. React. Kinet.* **1965**, *3*, 97. (c) Wolfgang, R. *Adv. High Temp. Chem.* **1971**, *4*, 43. (d) Skell, P. S.; Havel, J.; McGlinchey, M. J. *Acc. Chem. Res.* **1973**, *6*, 97. (e) Shevlin, P. B. In *Reactive Intermediates*, Vol. I; Abramovitch, R. A., Ed.; Plenum Press: New York, 1980; p 1.
(4) Kaiser, R. I.; Mebel, A. M. *Int. Rev. Phys. Chem.* **2002**, *21*, 307.
(5) Loison, J.-C.; Bergeat, A. *Phys. Chem. Chem. Phys.* **2004**, *6*, 5396.
(6) Clary, D. C.; Buonomo, E.; Sims, I. R.; Smith, I. W. M.; Geppert, W. D.; Naulin, C.; Costes, M.; Cartechini, L.; Casavecchia, P. *J. Phys. Chem. A* **2002**, *106*, 5541.
(7) Su, H.-F.; Kaiser, R. I.; Chang, A. H. H. *J. Chem. Phys.* **2005**, *122*, 074320.
(8) Geise, C. M.; Hadad, C. M.; Zheng, F.; Shevlin, P. B. *J. Am. Chem. Soc.* **2002**, *124*, 355.
(9) *Carbene Chemistry: From Fleeting Intermediates to Powerful Reagents*; Bertrand, G., Ed.; Marcel Dekker: New York, 2002.

 10.1021/ja060216m CCC: $33.50

potential energy surfaces, no ketene has been isolated. While the existence of an intermediate ketene was confirmed by the formation of pentanoic acid by the reaction with H_2O in the process of the reaction of arc-generated carbon with butanal,[10] the major products of the reaction of arc-generated carbon with carbonyl compounds come from carbenes which are formed from deoxygenation of the carbonyl compounds. Although C═C double bond cleavage in ketene is highly endothermic, this reaction is still feasible because of the high exothermicity of the initial reaction.

It is well established that deoxygenation occurs in the reaction of C (^{1}D) atoms with ketones and aldehydes.[1,10−16] Furthermore, it has been suggested that singlet excited-state ($^1B_1$) carbenes form in the C (^{1}D) atom deoxygenation of formaldehyde[13] and cyclopentanone.[16] The C atom deoxygenation of formaldehyde was reported in 1983 by Shevlin, where the generated carbene was allowed to react with (*Z*)-2-butene. After assessing the stereochemistry of the product mixture, the formation of CH_2 ($^1B_1$) was suggested.[13] However, the excited singlet carbene in this deoxygenation process was not observed, and it is still not clear how it can form.

Numerous studies of the CH_2CO potential energy surface (PES) have been reported,[17−23] including electronic states, photodissociation pathways, and oxirene rearrangements. However, a comprehensive studies of the PES for CH_2O + C is lacking. Hereupon, we report a computational study of C atom reactions in the ground state (^{3}P) and first excited state (^{1}D) with formaldehyde.

Computational Details

The Gaussian03 program[24] was used for the hybrid density functional PBE1PBE[25] calculations, while the GAMESS program[26] was used for Complete Active Space SCF (CASSCF)[27] and MCQDPT2[28] calculations. Geometry optimizations for minima and transition states were carried out at the (U)PBE1PBE/6-311++G(3df,p) (DFT) and CASSCF-(14,13)/6-311+G(2d,p) (CAS) levels. At the DFT level, harmonic vibrational analysis was performed and the minima and transition states were characterized. Thermodynamic correction terms, zero-point vibrational energies (ZPC), heat capacity corrections, and entropies (at 298 K) were obtained at the DFT level. Transition vectors of transition states were visualized by the MOLDEN program,[29] and if necessary, IRC calculations were carried out to connect the transition state to the corresponding minima.

For CASSCF geometry optimization, a (14,13) active space (14 electrons in 13 orbitals) was chosen from the full (16,14) valence active space of CH_2CO. To maintain a consistent active space, we included all valence electrons except for the oxygen lone pair that lies lowest in energy. For the product fragments, we considered the same orbitals so that the total active space was maintained as in CH_2CO. For example, a (6,6) active space was used for CH_2 and a (8,7) active space was used for CO.

At each stationary point at the CAS level, single-point energy calculations were carried out at the MCQDPT2/6-311+G(2d,p) (MCPT) level. Since the (14,13) active space calculations at the MCPT level are very challenging in terms of computing resources and computing cost, a (12,11) active space was used, where one low-lying C−H bonding orbital and its antibonding orbital were excluded. The active space of product fragments was chosen in the same way as at the CAS level (a (4,4) active space for CH_2 and a (8,7) active space for CO). The potential energy surfaces were constructed at the MCPT level with zero-point energy correction, heat capacity correction, and free energy correction calculated at the DFT level. The singlet and triplet surfaces are considered separately, and possible singlet−triplet crossings are not considered in this study. Further wave function analysis was carried out with CASSCF wave functions to examine correlations between the reaction intermediates and the products. We will use a notation scheme with a boldface "**S**" for singlets and "**T**" for triplets followed by one number for minima and two numbers or one number and a character for transition states. Thus, **S12** is the singlet transition state between **S1** and **S2** and **T5p** is the transition state between **T5** and products. We have not used the same numbering system between singlets and triplets, i.e., **S3** is a carbene while **T3** is the oxirene. A computational study of the ketene plus (*Z*)-2-butene reaction was carried out at the PBE1PBE/6-311+G(2d,p) level in an effort to rationalize the observed trapped products.

Result and Discussion

The structural isomers of CH_2CO in the singlet and triplet states at the DFT and CAS level are given in Figures 1 and 2. The calculated electronic energies and thermodynamic correction terms and spin-squared values are listed in Table 1. Numerous theoretical calculations on electronic states and photodissociation paths of CH_2CO have been reported.[17−23] The obtained geometric parameters in this study are in good agreement with those available in the literature,[17−23] which are not given in Figures 1 and 2 for reasons of clarity. The geometries of **S2** ($^1A_1$), **S4** ($^1A_1$), **T2** ($^3A''$), and **T2p** ($^3A''$) optimized at the DFT and CAS levels show good agreement with previous studies by East,[19b] Schaefer,[18b,23a] and Nemes.[19c] The C═C bond of **S2** is shorter than a normal double bond distance due to the electron

(10) Dewar, M. J. S.; Nelson, D. J.; Shevlin, P. B.; Biesiada, K. A. *J. Am. Chem. Soc.* **1981**, *103*, 2802.
(11) Skell, P. S.; Plonka, J. H. *J. Am. Chem. Soc.* **1970**, *92*, 836.
(12) Skell, P. S.; Plonka, J. H. *J. Am. Chem. Soc.* **1970**, *92*, 2160.
(13) Ahmed, S. N.; Shevlin, P. B. *J. Am. Chem. Soc.* **1983**, *105*, 6488.
(14) Fox, J. M.; Scacheri, J. E. G.; Jones, K. G. L.; Jones, M., Jr.; Shevlin, P. B.; Armstrong, B.; Sztyrbicka, R. *Tetrahedron Lett.* **1992**, *33*, 5021.
(15) Armstrong B. M.; McKee, M. L.; Shevlin, P. B. *J. Am. Chem. Soc.* **1995**, *117*, 3685.
(16) Xu, G.; Chang, T.-M.; Zhou, J.; McKee, M. L.; Shevlin, P. B. *J. Am. Chem. Soc.* **1999**, *121*, 7150.
(17) (a) Basch, H. *Theor. Chim. Acta* **1973**, *28*, 151. (b) Pendergast, P.; Fink, W. H. *J. Am. Chem. Soc.* **1976**, *98*, 648.
(18) (a) Yamabe, S.; Morokuma, K. *J. Am. Chem. Soc.* **1978**, *100*, 7551. (b) Allen, W. D.; Schaefer, H. F., III. *J. Chem. Phys.* **1988**, *89*, 329. (c) Klippenstein S. J.; East, A. L. L.; Allen, W. D. *J. Chem. Phys.* **1996**, *105*, 118.
(19) (a) Allen, W. D.; Schaefer, H. F., III. *J. Chem. Phys.* **1986**, *84*, 2212. (b) East, A. L. L.; Allen, W. D.; Klippenstein S. J. *J. Chem.* Phys. **1995**, *102*, 8506. (c) Szalay, P. G.; Császár, A. G.; Nemes, L. *J. Chem. Phys.* **1996**, *105*, 1034.
(20) Bouma, W. J.; Nobes, R. H.; Radom, L.; Woodward, C. E. *J. Org. Chem.* **1982**, *47*, 1869.
(21) Takeshita, K. *J. Chem. Phys.* **1992**, *96*, 1199.
(22) (a) Yoshimine, M. *J. Chem. Phys.* **1989**, *90*, 378. (b) Maier, G.; Reisenauer, H. P.; Cibulka, M. *Angew. Chem., Int. Ed.*. **1999**, *38*, 105. (c) Delamere, C.; Jakins, C.; Lewars, E. *THEOCHEM* **2002**, *593*, 79.
(23) (a) Scott, A. P.; Nobes, R. H.; Schaefer, H. F., III; Radom, L. *J. Am. Chem. Soc.* **1994**, *116*, 10159. (b) Delamere, C.; Jakins, C.; Lewars, E. *Can. J. Chem.* **2002**, *80*, 94. (c) Wilson, P. J.; Tozer, D. J. *Chem. Phys. Lett.* **2002**, *352*, 540. (d) Mawhinney, R. C. Goddard, J. D. *THEOCHEM* **2003**, *629*, 263. (e) Girard, Y.; Chaquin, P. *J. Phys. Chem. A* **2003**, *107*, 10462. (f) Zeller, K.-P.; Blocher, A.; Haiss, P. *Mini-Rev. Org. Chem.* **2004**, *1*, 291. (g) Kunioshi, N.; Yatabe, Y.; Mouri, S.; Fukutani, S. *JSME Int. J., Ser. B* **2000**, *43*, 258.
(24) Frisch, M. J.; et al. *Gaussian03*, Revision B.4; Gaussian, Inc.: Pittsburgh, PA, 2003.
(25) (a) Perdew, J. P.; Burke, K.; Ernzerhof, M. *Phys. Rev. Lett.* **1996**, *77*, 3865. (b) Perdew, J. P.; Burke, K.; Ernzerhof, M. *Phys. Rev. Lett.* **1997**, *78*, 1396.
(26) GAMESS: Schmidt, M. W.; Baldridge, K. K.; Boatz, J. A.; Elbert, S. T.; Gordon, M. S.; Jensen, J. J.; Koseki, S.; Matsunaga, N.; Nguyen, K. A.; Su, S.; Windus, T. L.; Dupuis, M.; Montgomery, J. A. *J. Comput. Chem.* **1993**, *14*, 1347.
(27) (a) Roos, B. O. The complete active space self-consistent field method and its applications in electronic structure calculations. In *Advances in Chemical Physics; Ab Initio Methods in Quantum Chemistry II*; Lawley, K. P., Ed.; John Wiley: Chichester, UK, 1987. (b) Schmidt, M. W.; Gordon, M. S. *Annu. Rev. Phys. Chem.* **1998**, *49*, 233.
(28) (a) Nakano, H. *J. Chem. Phys.* **1993**, *99*, 7983. (b) Nakano, H. *Chem. Phys. Lett.* **1993**, *207*, 372.
(29) MOLDEN: Schaftenaar, G.; Noordik, J. H. *J. Comput.-Aided Mol. Design* **2000**, *14*, 123.

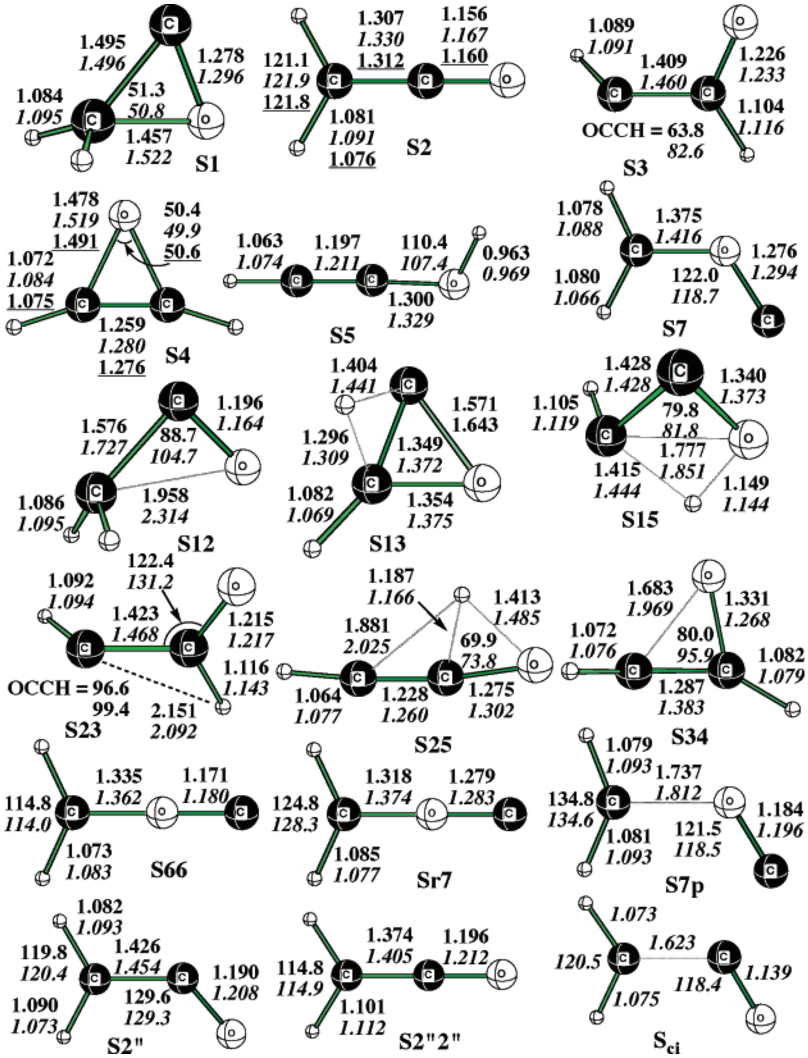

Figure 1. Optimized geometries of singlet species at the DFT (PBE1PBE/6-311++G(3df,p)) and CAS (CAS(14,13)/6-311+G(2d,p)) (in italic) levels. Literature values (underlined) for **S2** and **S4** are from refs 19b and 23a, respectively. The $\mathbf{S}_{\mathrm{ci}}$ (surface crossing) geometry was obtained at the CASSCF-(6,6)/6-311+G(2d,p) level. Bond lengths are in angstroms and angles are in degrees.

delocalization over the C−C−O π bonding system. On the triplet surface, **T2** is the lowest-energy structure, with a normal C−C single bond distance of 1.432 Å and a C−C−O angle of 127.9°. The C−O bond length of **T2** is about 0.03 Å longer than that in **S2**. However, the C−H distances are very similar in **S2** and **T2**. Triplet **T22′** ($^3A_2$) has the same atomic arrangement as **S2**; its C−O and C−C bond lengths are longer than those of **S2** (0.049 and 0.081 Å longer, respectively). The C atom end-on attack structures, **S66** ($^1A_1$), **Sr7** ($^1A_2$), and **T55** ($^3A_2$), are found to be transition states with one imaginary frequency and display distinct structural characteristics. Singlet **S66** has the shortest C−O bond length (1.180 Å) and the longest C−C bond (1.362 Å), while the structures of **Sr7** and **T55** are rather similar to each other. The stationary structures **Sr7** and **S7p** have two imaginary frequencies, and **S7** has one imaginary frequency. Distortions along the smaller imaginary frequency, which is out-of-plane bending, lead to real transition states or minimum with lower symmetry at the DFT level. However, the stationary points are close to the higher-symmetry species and, after zero-point correction, the higher-symmetry species are lower in energy. Thus, we considered **Sr7** and **S7p** as transition states and **S7** as a minimum despite the wrong number of imaginary frequencies and used the higher-symmetry structures for geometry optimization at the CAS level. The singlet and triplet carbene (**S3** and **T4**) intermediates are also characterized. Structurally, both are similar except that **S3** has an OCCH dihedral angle of 82.6° while **T4** is planar. On the singlet surface, several carbenes similar to **S3** are identified at the DFT level; among them, we chose the one with the lowest free energy for CAS-level thermodynamic corrections. The geometries of four lowest-energy states of methylene ($^3B_1$, $^1A_1$, $^1B_1$, and c^1A_1, Figure 3) are close to those reported in the literature.[30,31]

Calculated relative energies (kcal/mol) are given in Tables 2 and 3 for triplet and singlet species, respectively, and the schematic free energy surfaces for each multiplicity are given in Figures 4 and 5. In the discussion, we will use ΔG_{298}, which is the MCPT electronic energy, with ZPC, heat capacity (C_p), and entropy (ΔS) corrections at the DFT level. On the triplet free energy surface (Figure 4), **T2** is the lowest-energy species, −91.1 kcal/mol relative to CH_2O + C (^3P). The addition of a

(30) Petek, H.; Nesbitt, D. J.; Darwin, D. C.; Ogilby, P. R.; Moore, C. B.; Ramsay, D. A. *J. Chem. Phys.* **1989**, *91*, 6566.
(31) (a) Yamaguchi, Y. Sherrill, C. D.; Schaefer, H. F., III. *J. Phys. Chem.* **1996**, *100*, 7911. (b) Yamaguchi, Y.; Schaefer, H. F., III. *Chem. Phys.* **1997**, *225*, 23. (c) Jensen, P.; Bunker, P. R. *J. Chem. Phys.* **1988**, *89*, 1327. (d) Szabados, A.; Hargittai, M. *J. Phys. Chem. A* **2003**, *107*, 4314. (e) Kalemos, A.; Dunning, T. H., Jr.; Mavridis, A.; Harrison, J. F. *Can. J. Chem.* **2004**, *82*, 684.

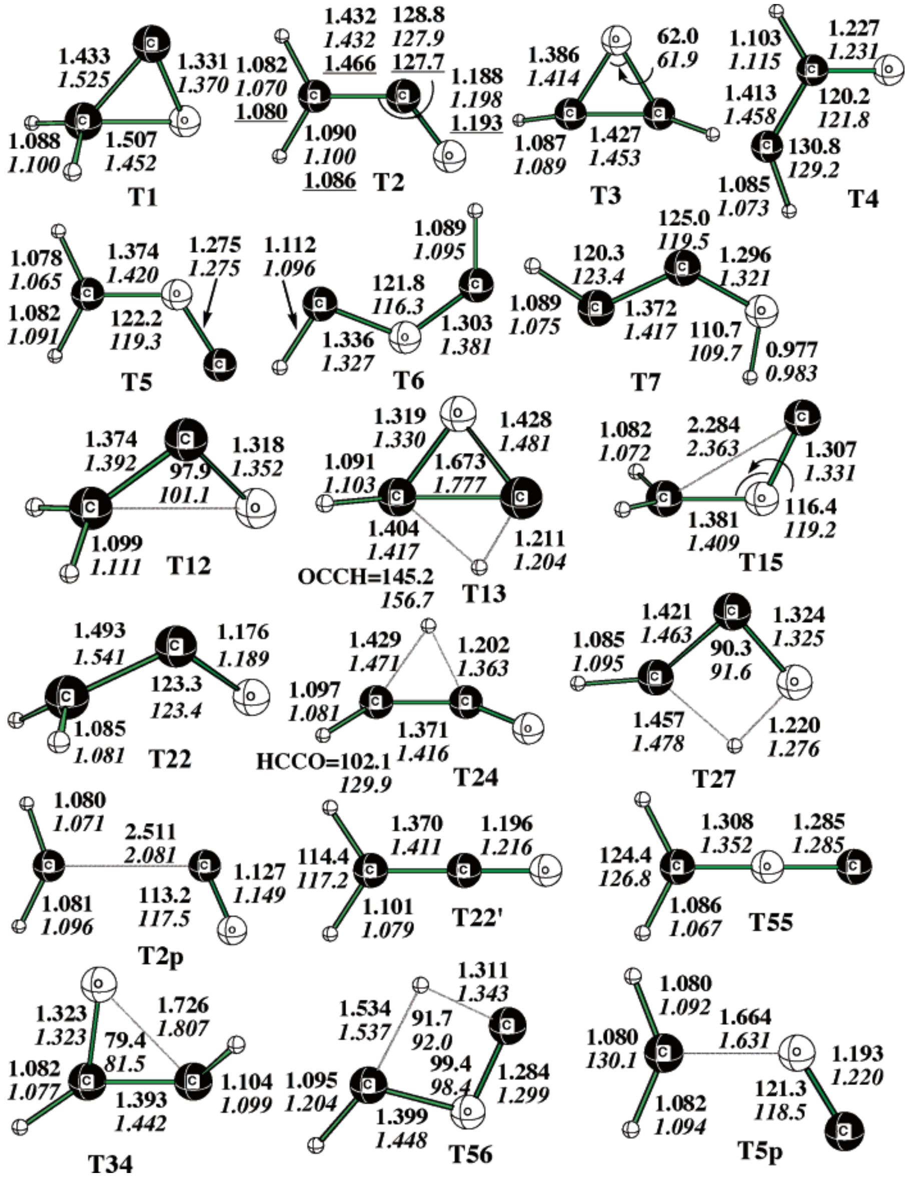

Figure 2. Optimized geometries of triplet species at the DFT (PBE1PBE/6-311++G(3df,p)) and CAS (CAS(14,13)/6-311+G(2d,p)) (in italic) levels. Literature values (underlined) for **T2** are from ref 18b. Bond lengths are in angstroms and angles are in degrees.

C atom to the C−O π bond initially forms a triplet oxiranylidene **T1** without barrier. **T1** can undergo H_2C−O bond-breaking, C−C bond-breaking, or hydrogen transfer to oxygen or to carbon. All four pathways were examined, but no transition state for hydrogen transfer to oxygen was found. The lowest-energy pathway leads to **T2** on the triplet surface, with a free energy barrier of 14.5 kcal/mol and a reaction free energy of −66.3 kcal/mol. There must be a valley−ridge inflection (VRI) points or a bifurcation along the H_2C−O bond-breaking (**T1** → **T2**),[33] because a C−O stretching mode cannot directly connect two minima (**T1** and **T2**); a rotation or bending mode is also necessary. At a VRI point along the C−C−O opening coordinate, the eigenvalue of the C−O stretching vector becomes zero and the rotational mode around the C−C bond becomes imaginary. Therefore, there are two saddle points along the C_s symmetry coordinate, **T12** with a C−O stretching transition vector and **T22** with a rotation transiton vector around the C−C bond.

Other dissociation pathways are not studied in detail. The free energies (298 K) of products show that, on the triplet free energy surface, the formation of CO plus methylene is the dominant pathway and the dissociation to oxygen (O(^{3}P)) and acetylene (−29.0 kcal/mol) is much higher in free energy than methylene formation (−78.2 kcal/mol). The hydrogen extrusion might be a competitive channel (−50.0 kcal/mol), and this would lead to other products. This part of the PES has already been studied in detail,[23f,g] and we are in good agreement with previous results.

Ketene **T2** can undergo two interconversions: a rotation around the C−C bond (8.5 kcal/mol free energy barrier) and an inversion via a linear C−C−O structure (**T22′**, 27.0 kcal/mol barrier). It is also possible to transfer a hydrogen atom to the other carbon to form a triplet carbene (**T4**), though the free energy barrier is quite unfavorable (58.0 kcal/mol). The fate of **T4** is not clear. Breaking the C−C bond to yield CH and HCO is very unfavorable (75.1 kcal/mol free energy barrier). There-

(32) Computational Chemistry Comparison and Benchmark Database (CCCBDB) at http://srdata.nist.gov/cccbdb/default.htm.

(33) (a) Castaño, O.; Frutos, L.-M.; Palmeiro, R.; Notario, R.; Andrés, J. L.; Gomperts, R.; Blancafort, L.; Robb, M. A. *Angew. Chem., Int. Ed.* **2000**, *39*, 2095. (b) Basilevsky, M. V. *Chem. Phys.* **1977**, *24*, 81. (c) Valtazanos, P.; Ruedenberg, K. *Theor. Chem. Acta* **1986**, *69*, 281.

Table 1. Calculated Electronic Energies (au) at the DFT, CAS, and MCPT Levels along with ZPC (kcal/mol), H_{corr} (kcal/mol), Entropy (S, cal/K·mol), DFT Spin-Squared Value ($\langle S^2 \rangle$), CAS Reference Weight of Dominant Configuration (c_i^2), and Electronic States

	ZPC	H_{corr}	S	$\langle S^2 \rangle$	c_i^2	state	DFT	CAS	MCPT
C (^{3}P)	0.0	1.5	35.6	2.00		^{3}P	−37.80321	−37.70299	−37.76948
C (^{1}D)	0.0	1.5	33.4	1.01		^{1}D	−37.78825	−37.64525	−37.71821
C (^{1}S)	0.0	1.5	33.4	0.00		^{1}S	−37.73128	−37.60755	−37.67319
CO	3.2	5.3	47.2	0.00		$^1\Sigma$	−113.22500	−112.90363	−113.09712
CH_2O	16.8	19.2	52.2	0.00		$^1A_1$	−114.41299	−114.03723	−114.25908
CH_2 ($^3B_1$)	10.9	13.3	46.6	2.01	0.97	$^3B_1$	−39.11334	−38.96922	−39.04985
CH_2 ($^1A_1$)	10.5	12.8	45.2	0.00	0.92	$^1A_1$	−39.08598	−38.95214	−39.02520
CH_2 ($^1B_1$)	10.8	13.2	45.0	0.79	0.48	$^1B_1$	−39.09191	−38.90222	−38.99299
CH_2 (c^1A_1)[a]	10.6	13.0	42.0		0.49	$^1A_1$		−38.85490	−38.95163
CH	4.1	6.2	42.3	0.75	0.49	$^2\Pi$	−38.43636	−38.31836	−38.38820
HCO	8.3	10.6	53.6	0.75	0.94	$^2A'$	−113.76579	−113.40462	−113.62390
S1	20.4	22.9	58.3	0.00	0.90	$^1A'$	−152.37894	−151.86774	−152.15813
S2	19.9	22.7	57.7	0.00	0.90	$^1A'$	−152.48037	−151.96541	−152.26748
S2″	19.6	22.3	59.5	1.02	0.40	$^1A''$	−152.39395	−151.86882	−152.17944
S3	17.6	20.9	63.4	0.66	0.86	^1A	−152.35063	−151.83978	−152.13372
S4	18.7	21.6	59.5	0.00	0.88	$^1A_1$	−152.35261	−151.82673	−152.14154
S5	20.1	23.1	59.0	0.00	0.90	$^1A'$	−152.42108	−151.90656	−152.21047
S6[b]	18.6	21.6	60.9	0.00		$^1A'$	−152.31492		
S7[c]	17.5	20.4	60.1	1.01	0.46	$^1A''$	−152.29307	−151.78186	−152.06890
S12	17.5	20.3	60.7	0.55	0.12	$^1A'$	−152.34339	−151.83313	−152.13225
S13	16.8	19.3	58.6	0.00	0.88	^1A	−152.29228	−151.76894	−152.07458
S15	15.8	18.4	58.8	0.00	0.89	^1A	−152.26001	−151.74954	−152.03200
S2″2″	18.0	20.6	57.1	1.02	0.31	$^1A_2$	−152.36022	−151.83125	−152.14786
S23	17.2	20.0	59.8	0.64	0.89	$^1A'$	−152.35024	−151.83890	−152.13009
S25	16.0	19.1	60.6	0.00	0.83	$^1A'$	−152.32577	−151.79756	−152.12003
S34	18.4	21.0	59.2	0.00	0.84	^1A	−152.35046	−151.84396	−152.13308
S66	18.4	21.2	57.9	0.00	0.87	$^1A_1$	−152.31127	−151.79402	−152.09282
S6p[b]	17.5	20.6	61.4	0.00		$^1A'$	−152.31396		
S7p[c]	15.9	19.2	64.0	1.00	0.41	$^1A'$	−152.27168	−151.73690	−152.05775
Sr7[c]	17.2	20.2	59.7	1.01	0.37	$^1A_2$	−152.26256	−151.73876	−152.03349
$\mathbf{S_{ci}}$[d]	19.6	22.3	59.5					−151.84950	−152.16824
T1	20.1	22.7	60.6	2.01	0.91	$^3A''$	−152.29621	−151.76542	−152.08428
T2	19.1	21.9	62.2	2.01	0.16	$^3A''$	−152.39793	−151.87873	−152.18798
T3	19.6	22.2	59.2	2.01	0.91	^3B	−152.32432	−151.78806	−152.10321
T4	19.0	21.7	61.9	2.03	0.90	$^3A''$	−152.36686	−151.85794	−152.15574
T5	17.9	21.0	63.5	2.01	0.06	$^3A''$	−152.29754	−151.79195	−152.07875
T6	17.1	20.1	63.5	2.01	0.90	$^3A''$	−152.24274	−151.74531	−152.02303
T7	19.0	21.8	62.0	2.01	0.84	$^3A''$	−152.31178	−151.77501	−152.10270
T12	19.6	22.0	60.5	2.13	0.03	$^3A''$	−152.26744	−151.73773	−152.06021
T13	16.3	18.9	60.8	2.01	0.89	^3A	−152.24172	−151.70055	−152.02343
T15	17.1	20.1	65.2	2.01	0.80	$^3A''$	−152.25769	−151.75622	−152.04323
T22	18.0	20.7	61.7	2.01	0.91	$^3A'$	−152.38049	−151.86024	−152.17257
T24	15.4	18.2	61.7	2.02	0.87	^3A	−152.30075	−151.77008	−152.08981
T27	15.0	17.7	61.4	2.02	0.51	$^3A''$	−152.23731	−151.71033	−152.02596
T2p	15.0	18.9	72.0	2.01	0.84	$^3A''$	−152.33779	−151.84749	−152.14815
T34	17.6	20.2	61.2	2.01	0.74	^3A	−152.28006	−151.75141	−152.07125
T56	15.0	17.7	61.5	2.02	0.84	$^3A''$	−152.22171	−151.69994	−152.02092
T5p	15.5	18.9	66.4	2.02	0.64	$^3A''$	−152.28497	−151.77296	−152.08015
T22′	18.0	20.7	59.2	2.01	0.91	$^3A_2$	−152.36096	−151.82249	−152.14431
T55	17.3	20.2	61.3	2.02	0.64	$^3A_2$	−152.26537	−151.71934	−152.03924

[a] Thermodynamic correction data are obtained at the CAS level, because we could not locate the excited c^1A_1 minimum at the DFT level. [b] At the CAS level, a stationary point for **S6p** could not be found. At the DFT level, after the zero-point energy correction, the relative energy order of the minimum (**S6**) and the transition state (**S6p**) becomes reversed. We conclude, therefore, that **S6** will not exist on the potential energy surface. [c] The three indicated structures have an "extra" imaginary frequency that corresponds to out-of-plane distortion. When the true transition states (**Sr7** and **S7p**) and minimum (**S7**) were located in C_1 symmetry at the DFT level, zero-point corrections reversed the relative energies with the corresponding higher-symmetry (C_s) structures. For that reason, C_s symmetry was used for the CAS level geometry optimization. [d] Single-point energy calculations at the CAS and MCPT levels are performed for both the $^1A'$ and $^1A''$ states on the geometry obtained from conical intersection optimization at the CAS(6,6)/6-311+G(2d,p) level. The energy reported is the average of both states. Thermodynamic corrections of **S2″** are used for the enthalpy and free energy corrections of the conical intersection structure.

fore, **T4** most likely will undergo reactions with reactants (i.e., CH_2O). The pathway we are most interested in for **T2** is breaking the C−C bond to form carbon monoxide and triplet-state methylene ($^3B_1$) with a 19.0 kcal/mol free energy barrier (reverse barrier, 6.1 kcal/mol). This result is in good agreement with those reported by Allen et al.[18b] The C−C bond dissociation energy (ΔH_0 = 20.7 kcal/mol, Table 2) is also close to their calculated value (18.6 kcal/mol) and the proposed value of 22.3 kcal/mol.[18b] The 0 K enthalpy barrier (forward, 20.9 kcal/mol; reverse, 0.2 kcal/mol) is somewhat lower than their estimation (forward, 25−27 kcal/mol; reverse, 3−4 kcal/mol). Thus, the reaction of triplet methylene with CO to form **T2** has a very low barrier.

In **T1**, hydrogen transfer to another carbon is not likely to occur due to a 34.3 kcal/mol free energy barrier. If C atoms have a large amount of kinetic energy, then this barrier could be overcome, which would lead to triplet oxirene, **T3**, which can transform into a carbene **T4**. If C−C bond cleavage occurs in **T1**, the bent $H_2C{-}O{-}C$ (**T5**) isomer will form. However, **T5** will dissociate into CO and CH_2 ($^3B_1$) without a free energy

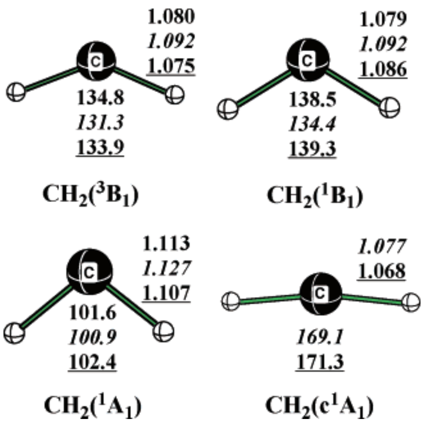

Figure 3. Optimized geometries of the four lowest energy states of methylenes at the DFT and CAS (in italic) levels. Literature values (underlined) are from ref 31. Bond lengths are in angstroms and angles are in degrees.

Table 2. Relative Enthalpies (kcal/mol) of C_2H_2O Triplet Isomers at 0 K (ΔH_0) and 298 K (ΔH_{298}) and Free Energies at 298 K (ΔG_{298}) Calculated at the MCPT Level with Thermodynamic Corrections at the DFT Level[a]

		ΔH_{298}		
	ΔH_0	calc	exp	ΔG_{298}
$CH_2O + C$ (^3P)	0.0	0.0	0.0	0.0
$CH_2O + C$ (^1D)	32.2	32.2	29.1[b]	32.8
$CH_2O + C$ (^1S)	60.4	60.4	61.9[b]	61.1
$CO + CH_2$ ($^3B_1$)	−77.0	−76.4	−76.7[c]	−78.2
$CO + CH_2$ ($^1A_1$)	−61.9	−61.3	−67.7[c]	−62.7
$CO + CH_2$ ($^1B_1$)	−41.4	−41.4	−43.8[c]	−42.3
$CO + CH_2$ (c^1A_1)	−18.8	−17.4	−16.6[c]	−15.8
CH + HCO	5.9	6.5	8.2[d]	4.1
T1	−31.6	−32.9		−24.8
T2	−97.7	−98.7		−91.1
T3	−44.0	−45.3		−36.8
T4	−77.5	−78.7		−71.0
T5	−30.4	−31.2		−23.9
T6	5.3	4.5		11.8
T7	−44.3	−45.4		−37.7
T12	−17.0	−18.5		−10.2
T13	2.8	1.4		9.5
T15	−8.9	−9.7		−3.0
T22	−89.1	−90.3		−82.6
T24	−39.8	−40.9		−33.1
T27	−0.1	−1.3		6.5
T2p	−76.8	−76.8		−72.1
T34	−25.9	−27.2		−19.3
T56	3.1	1.9		9.7
T5p	−33.6	−34.1		−27.7
Tv1	−71.4	−72.6		−64.1
n	−5.5	−6.5		0.8

[a] All thermodynamic values are relative to $CH_2O + C$ (^3P). [b] The experimental ΔH_{298} values for C (^3P) and CH_2O are taken as 171.3 and −27.7 kcal/mol, respectively. Relative energies are calculated by using the data from ref 2. [c] A value of 93.3 kcal/mol was used for ΔH_{298} of triplet methylene from ref 32. The energy separations $^3B_1-^1A_1$ (9.0 kcal/mol, ref 31b), $^3B_1-^1B_1$ (32.9 kcal/mol, ref 31c), and $^3B_1-c^1A_1$ (60.1 kcal/mol, ref 31a) were used to determine the ΔH_{298} of the excited states of methylene. [d] An experimental value of 10.0 kcal/mol for the ΔH_{298} of CHO was used from ref 32.

barrier. **T5p** was located as a transition state at both the DFT and CAS levels, but at the MCPT level the energy is lower than that of **T5**. A transition state **T55** was located as the inversion transition for **T5**.

It is known experimentally that triplet C atoms abstract hydrogen atoms from organic compounds.[1] On this surface, no transition state could be located for hydrogen abstraction, which is nonspontaneous ($\Delta G_{298} = 4.1$ kcal/mol) and proceeds without

Table 3. Relative Enthalpies (kcal/mol) of C_2H_2O Singlet Isomers at 0 K (ΔH_0) and 298 K (ΔH_{298}) and Free Energies at 298 K (ΔG_{298}) Calculated at the MCPT Level with Thermodynamic Corrections at the DFT Level[a]

		ΔH_{298}		
	ΔH_0	calc	exp	ΔG_{298}
$CH_2O + C$ (^3P)	0.0	0.0	0.0	0.0
$CH_2O + C$ (^1D)	32.2	32.2	29.1	32.8
$CH_2O + C$ (^1S)	60.4	60.4	61.9	61.1
$CO + CH_2$ ($^3B_1$)	−77.0	−76.4	−76.7	−78.2
$CO + CH_2$ ($^1A_1$)	−61.9	−61.3	−67.7	−62.7
$CO + CH_2$ ($^1B_1$)	−41.4	−41.4	−43.8	−42.3
$CO + CH_2$ (c^1A_1)	−18.8	−17.4	−16.6	−15.8
CH ($^2\Pi$) + HCO ($^2A'$)	5.9	6.5	8.2	4.1
S1	−77.7	−79.0		−70.2
S2	−146.8	−147.9	−155.0[b]	−138.9
S2″	−91.9	−93.0		−84.6
S3	−65.1	−65.7		−58.5
S4	−69.0	−69.9		−61.5
S5	−110.8	−111.7		−103.1
S7	−25.7	−26.8		−18.5
S12	−64.4	−65.4		−57.3
S13	−28.9	−30.2		−21.5
S15	−3.1	−4.4		4.2
S23	−63.2	−64.4		−56.0
S25	−58.2	−58.9		−50.8
S34	−64.0	−65.2		−56.7
S66	−38.7	−39.8		−30.8
S7p	−19.1	−19.7		−12.6
Sr7	−2.7	−3.5		4.9
$\mathbf{S_{ci}}$	−84.8	−86.0		−77.5

[a] All thermodynamic values are relative to $CH_2O + C$ (^3P). For the detailed explanation, see Table 2. [b] A value of 11.4 kcal/mol from ref 32 was used for ΔH_{298} of the ground state of ketene (**S2**) to calculate relative enthalpies.

a reverse barrier. There is ample evidence that C−H abstractions by radicals have low activation barriers. For example, hydrogen abstractions from formaldehyde by halogen atoms are almost barrierless (for Cl) at the CCSD(T)//B3LYP/6-311++G(d,p) level[34a] and have very low barriers (8.5 and 4.4 kcal/mol for F and Cl, respectively) at the MP2/aug-cc-pVDZ level.[34b] In this context, it is not surprising that the hydrogen abstraction from formaldehyde by C (^3P) proceeds without reverse barrier. In addition, as shown in eq 2, no electron rearrangement is necessary to produce two ground-state products in this reaction.

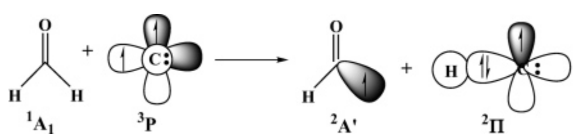

(2)

On the singlet PES (Figure 5), the most probable reaction between C (^1D) with formaldehyde is also π addition to form **S1**. This reaction is 103.0 kcal/mol exoergic, and **S1** will have enough energy to undergo further reaction. The lowest energy reaction path is to form ground state **S2** ($^1A_1$) via **S12** over a 12.9 kcal/mol free energy barrier by breaking the H_2C-O bond. Another possible path is hydrogen transfer to either carbon or oxygen. Although hydrogen transfer to carbon has a high barrier (48.7 kcal/mol), the system has enough energy to yield singlet carbene **S3**. The singlet carbene, **S3**, can easily convert into **S2** (2.5 kcal/mol barrier). It can also make a C−O bond to form oxirene, **S4**. Our results are in good agreement with a number

(34) (a) Dong, F.; Qu, Z.; Zhang, Q.; Kong, F. *Chem. Phys. Lett.* **2003**, *371*, 29. (b) Beukes, J. A.; D'Anna, B.; Nielsen, C. J. *Phys. Chem. Chem. Phys.* **2000**, *2*, 4049.

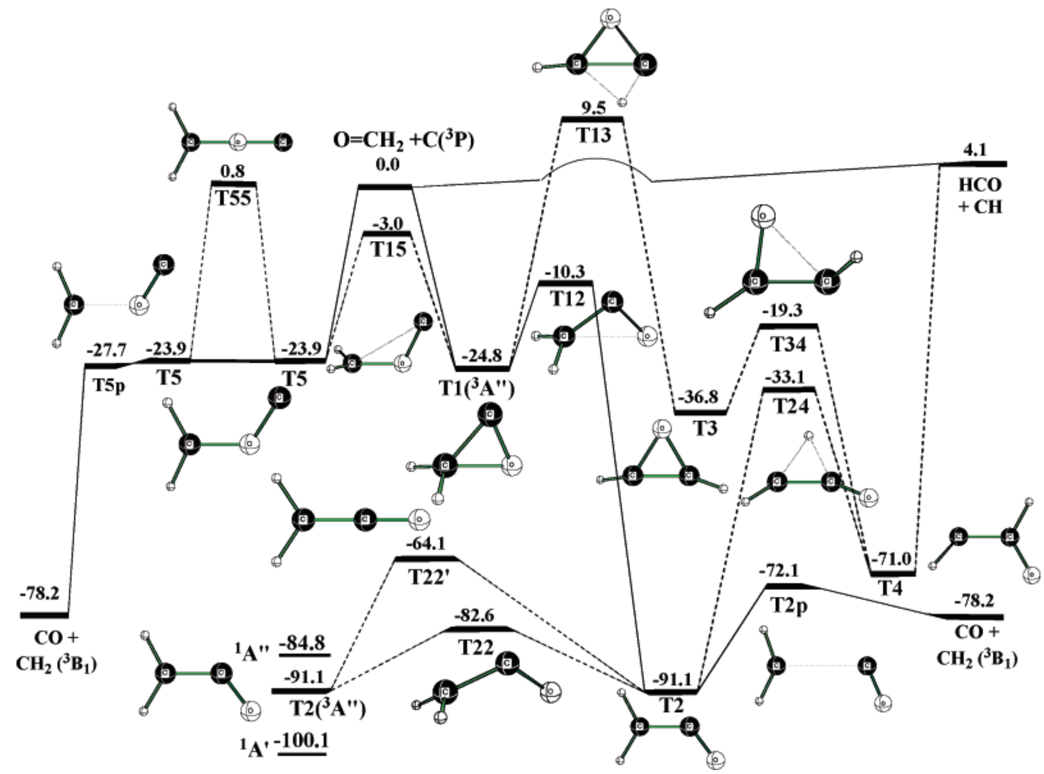

Figure 4. Triplet free energy surface constructed from ΔG_{298} at the MCPT level. The free energies of singlet H_2CCO ($^1A''$ and $^1A'$) are computed at the **T2**($^3A''$) geometry. Relative energies are given in kilocalories per mole.

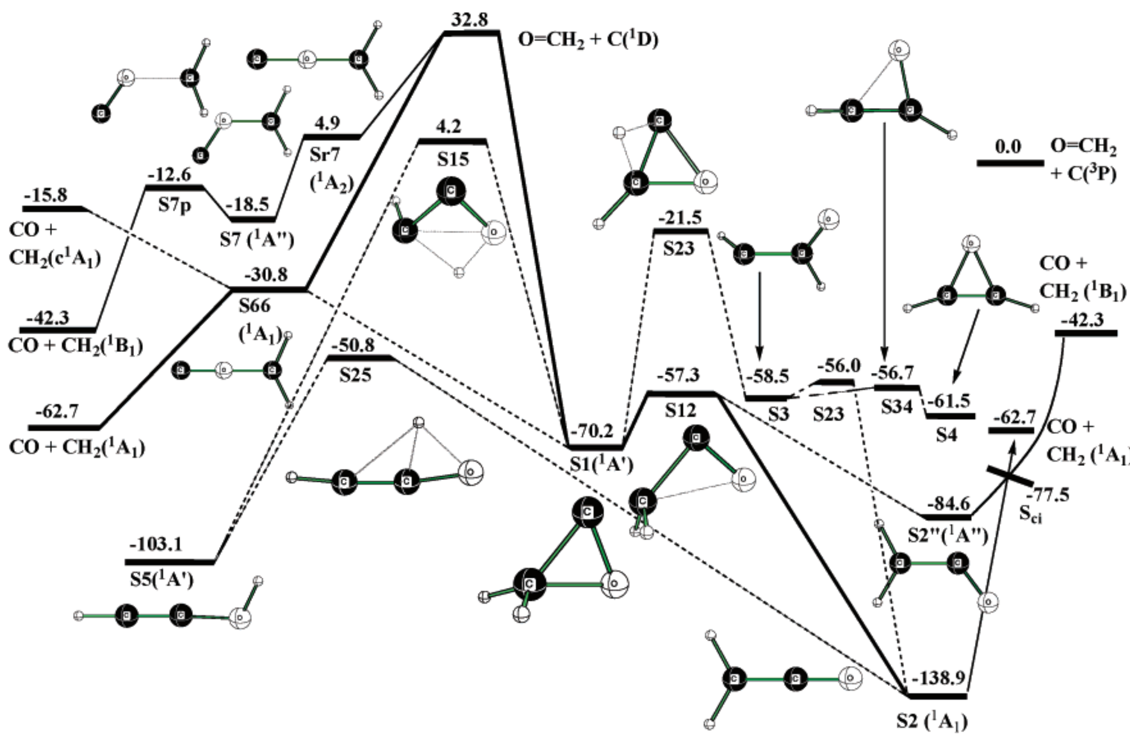

Figure 5. Singlet free energy surface constructed from ΔG_{298} at the MCPT level. S_{ci} is the crossing geometry between the $^1A'$ and $^1A''$ surfaces (see text). Relative energies are given in kilocalories per mole.

of studies which have been performed on the singlet oxirene rearrangement mechanism (Wolff rearrangement).[23] Singlet **S3** is lower than **S4** in free energy at the CAS level, but the energy order is reversed at the MCPT level. A similar disagreement has been reported between the MP2 and CCSD(T) levels, where the singlet carbene (**S3**) is a minimum at the CCSD(T) level but not at the MP2 level.[23b,e] The authors[23e] felt that truncation after the second-order term in perturbation theory was responsible for the poor description of the singlet carbene, **S3**.

In **S1**, hydrogen transfer to oxygen to form **S5** has a high free energy barrier (74.4 kcal/mol). Singlet **S5** has a collinear H−C−C−O arrangement, and it is the second lowest species on the free energy surface. A transition state between **S2** and **S5** has also been located. Surprisingly, a hydrogen atom moves directly from oxygen to the end carbon without forming an intervening intermediate. The thermodynamic advantage of making a C═O double bond might be the driving force of this process at the expense of a C≡C triple bond.

In **S1**, the C−C bond-breaking process is complicated. Opening the C−C bond will lead to **S66** ($^1A_1$), which has an out-of-plane bending mode of two hydrogen atoms as a transition vector. At the DFT level, a minimum and a transition state were located, but after zero-point energy corrections, the transition state has a lower energy than the minimum. At the CAS level, no minimum was located, and distortion along the transition vector led directly to dissociation of ketene to CO + CH_2 ($^1A_1$). Another way to form **S66** is direct addition of the C atom to oxygen. This pathway has no barrier and will lead to either the $^1A_1$ methylene (+CO) or **S1**.

On the singlet PES, two pathways which lead to formation of the $^1B_1$ methylene were found. One starts from direct attack of C (^1D) on oxygen to form **Sr7** ($^1A_2$), which is a transition state for interconversion of **S7** ($^1A''$). Singlet **S7** dissociates via a 5.9 kcal/mol free energy barrier to give CO and singlet excited methylene ($^1B_1$). These three (**Sr7**, **S7**, and **S7p**) are biradical species on the $^1A''$ surface.

The central question is whether $^1B_1$ methylene can be formed on the $^1A''$ surface. The ^1D state has five microstates which will split into two A_1 and one A_2, B_1, and B_2 states in C_{2v} symmetry, and into three A′ and two A″ states in C_s symmetry. When the ^1D carbon attacks the formaldehyde oxygen atom, the microstates will split into three $^1A'$ and two $^1A''$ states, and the ratio between states of A′ and A″ symmetry will be 3:2. Thus, reactions on the A″ surface are certainly possible. The next question to consider is whether this deoxygenation process is faster than intersystem crossing (ISC). The quantitative answer to this question cannot be obtained from this study, but it can be answered qualitatively. The dissociation will proceed very quickly, since it has only a 5.9 kcal/mol barrier, and the system will have about 50 kcal/mol extra energy at **S7**. The ISC occurs along the seam of two potential energy surfaces if the spin−orbit coupling is large enough and the geometries are similar to each other.[35−39] Generally speaking, the spin−orbit coupling is large in heavier elements, but in the first-row elements the spin−orbit coupling is very small.[36,38] One example of a triplet−singlet intersystem crossing rate has been reported in CF_2CF_2−O as 4×10^{12} s^{-1}.[40] The rate of ISC in $COCH_2$ may be similar to that in CF_2CF_2−O since the energy gap between the $^1A''$ and $^3A''$ surfaces is also small (**S7**−**T5**: $\Delta G = 5.4$ kcal/mol, from Tables 2 and 3). Thus, the excited singlet species ($^1A''$) should undergo rapid ISC to the lower $^3A''$ surface. However, F_2CF_2-CO differs from $CH_2(^1B_1)$ in that it is a biradical with a radical center on oxygen, and this factor may be responsible for the rapid ISC observed in this species. In the present reaction, we suggest that the formation of $^1B_1$ methylene via the $^1A''$ surface (**Sr7** → **S7** → **S7p**) can occur only if ISC is slow relative to dissociation. Therefore, we suggest that the formation of $^1B_1$ methylene via the $^1A''$ surface (**Sr7** → **S7** → **S7p**), while possible, should not be a significant process.

The other pathway, which proceeds along a $^1A''$ surface (**S2″** ($^1A''$) → CO + $CH_2(^1B_1)$), starts at **S12**, a biradical stationary point of $^1A'$ symmetry with strong multireferential character, and breaks symmetry as the reaction proceeds to **S2″**. While **S12** is a transition state at the DFT level, we explored the possibility that **S12** might be a second-order stationary point at the CAS level. We optimized the **S12** geometry at the CAS(12,11)/6-311+G(2d,p) level and computed numerical vibrational frequencies. At this level, **S12** was found to be a second-order saddle point with two distinct imaginary frequencies (a′, 320i; a″, 164i). Stretching the H_2C−O bond in **S12** leads to the global minimum **S2**, while rotating around the C−C bond leads to **S2″** ($^1A''$ state). The **S2″** open-shell carbene is the lowest free-energy species on the $^1A''$ surface and will lead to $^1B_1$ methylene with a 42.3 free energy barrier.

Along the C−C bond-breaking pathway (**S2″** → CO + $CH_2(^1B_1)$), a conical intersection $\mathbf{S}_{ci}$ between the $^1A'$ and $^1A''$ surfaces was found using the CAS(6,6)/6-311+G(2d,p) method. The conical intersection is lower in free energy by 14.8 kcal/mol than the CH_2 ($^1A_1$) plus CO. This conical intersection allows radiationless decay of **S2″** to **S2**. However, if the bond-breaking process of **S2″** is fast, it is possible to pass through the conical intersection to form CH_2 ($^1B_1$) plus CO, in accordance with Carpenter's nonstatistical dynamic effect.[41]

It is still not clear if the products observed from C (^1D) and formaledhyde could come from other lower-energy intermediates on the singlet PES. Thus, we examined orbital correlations

Table 4. Important Valence Electron Configurations of the Four Lowest Electronic State Methylenes and Four Singlet Species Obtained at the CAS Level

	configuration	$\lvert c_i \rvert^b$
CH_2 ($^3B_1$)	$a_1^2b_2^2a_1b_1$	0.98
CH_2 ($^1A_1$)	$a_1^2b_2^2a_1^2$	0.97
	$a_1^2b_2^2b_1^2$	0.18
CH_2 ($^1B_1$)	$a_1^2b_2^2a_1\bar{b}_1$	0.70
	$a_1^2b_2^2\bar{a}_1b_1$	0.70
CH_2 (c^1A_1)	$a_1^2b_2^2b_1^2$	0.73
	$a_1^2b_2^2a_1^2$	0.67
S2 ($^1A_1$)	$a_1^2a_1^2b_2^2a_1^2a_1^2b_1^2b_2^2b_1^2$	0.95
	$a_1^2a_1^2b_2^2a_1^2a_1^2b_1^2b_1^2b_2^2$	0.12
	$a_1^2a_1^2b_2^2a_1^2a_1^2b_1^2b_2^2b_1^2$	0.10
S2″ ($^1A''$)	$a'^2a'^2a'^2a'^2a'^2a''^2a'^2a''\bar{a}'$	0.63
	$a'^2a'^2a'^2a'^2a'^2a''^2a'^2\bar{a}''a'$	0.63
	$a'^2a'^2a'^2a'^2a'^2a''^2a'^2\bar{a}'a''$	0.17
	$a'^2a'^2a'^2a'^2a'^2a''^2a'^2a'\bar{a}''$	0.17
S66 ($^1A_1$)	$a_1^2a_1^2b_2^2a_1^2b_1^2a_1^2b_2^2b_1^2$	0.93
	$a_1^2a_1^2b_2^2a_1^2b_1^2a_1^2b_2^2b_2^2$	0.15
Sr7 ($^1A_2$)	$a_1^2a_1^2a_1^2b_2^2b_1^2a_1^2b_2^2b_1\bar{b}_2$	0.61
	$a_1^2a_1^2a_1^2b_2^2b_1^2a_1^2b_2^2\bar{b}_1b_2$	0.61
	$a_1^2a_1^2a_1^2b_2^2b_1^2a_1^2b_2^2b_1\bar{b}_2$	0.29
	$a_1^2a_1^2a_1^2b_2^2b_1^2a_1^2b_2^2\bar{b}_1b_2$	0.29
S7p ($^1A''$)	$a'^2a'^2a'^2a''^2a'^2a'^2a'^2a'\bar{a}''$	0.64
	$a'^2a'^2a'^2a''^2a'^2a'^2a'^2\bar{a}'a''$	0.64
	$a'^2a'^2a'^2a''^2a'^2a'^2a'^2a'\bar{a}''$	0.17
	$a'^2a'^2a'^2a''^2a'^2a'^2a'^2\bar{a}'a''$	0.17

[a] For clarity, core electron configurations are omitted. Singly occupied β orbitals are designated with a bar over the orbital designation. [b] Absolute value of coefficient of each configuration.

(35) Turro, N. J.; Cha, Y.; Gould, I. R. *J. Am. Chem. Soc.* **1987**, *109*, 2101.
(36) Hoffmann, M. R.; Schatz, G. C. *J. Chem. Phys.* **2000**, *113*, 9456.
(37) Biczók, L.; Bérces, T.; Yatsuhashi, T.; Tachibana, H.; Inoue, H. *Phys. Chem. Chem. Phys.* **2001**, *3*, 980.
(38) Byeon, C. C.; McKerns, M. M.; Sun, W.; Nordlund, T. M.; Lawson, C. M.; Gray, G. M. *Appl. Phys. Lett.* **2004**, *84*, 5174.
(39) Blitz, M. A.; Pilling, M. J.; Seakins, P. W. *Phys. Chem. Chem. Phys.* **2001**, *3*, 2241.
(40) Nguyen, T. L.; Dils, B.; Carl, S. A.; Vereecken, L.; Peeters, J. *J. Phys. Chem. A* **2005**, *109*, 9786.

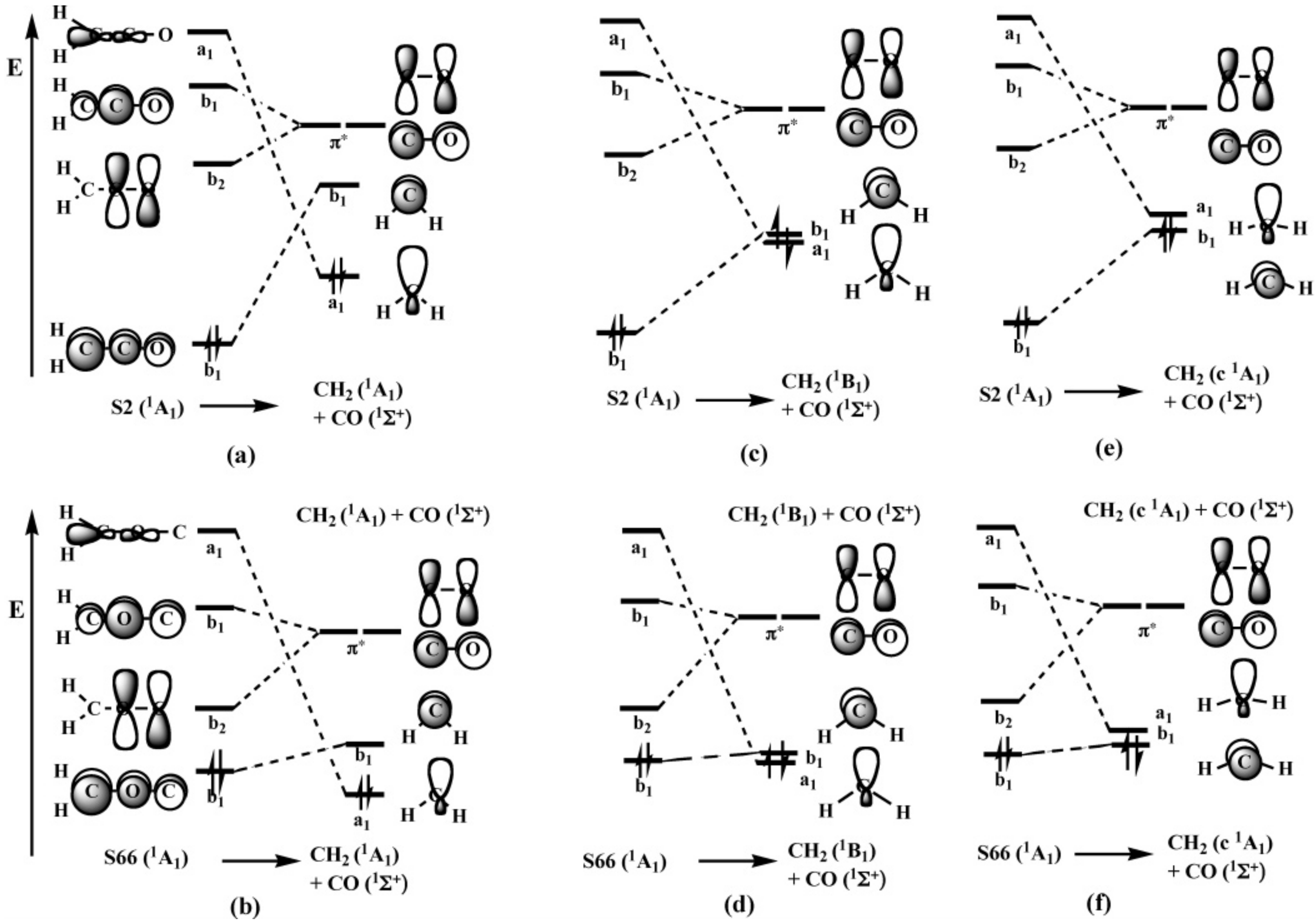

Figure 6. Orbital crossing diagram for the singlet methylene-producing reactions from **S2** and **S66**. (a) **S2** → CO + CH_2 ($^1A_1$), (b) **S66** → CO + CH_2 ($^1A_1$), (c) **S2** → CO + CH_2 ($^1B_1$), (d) **S66** → CO + CH_2 ($^1B_1$), (e) **S2** → CO + CH_2 (c^1A_1), and (f) **S66** → CO + CH_2 (c^1A_1).

between ketene with C_{2v} symmetry (**S2** and **S66**) and carbene products (Figure 6). Their valence electron configurations are given in Table 4. Interestingly, neither **S2** nor **S66** directly correlates to the lowest $^1A_1$ state methylene plus CO, but both correlate to the third excited c^1A_1 state methylene plus CO. As the C−C (C−O) distance becomes longer in **S2 (S66)**, the C−C antibonding orbital (a_1) will be stabilized, but the occupied b_1 orbital will be destabilized due to the loss of π bonding interaction. As shown in Figure 6, to correlate the $^1A_1$ ketene (**S1** or **S66**) with the $^1A_1$ methylene plus CO, the orbital crossing between b_1 and a_1 orbitals is unavoidable. The correlation diagram between the $^1A_1$ ketene state and the $^1B_1$ methylene state plus CO (Figure 6c,d) also shows a crossing, but the energies of the two orbitals (a_1 and b_1) are pseudo-degenerate. The $^1A_1$ state ketene isomers, **S2** and **S66**, correlate with the excited c^1A_1 methylene plus CO without orbital crossing (Figure 6e,f). In this case, there must be a transition state in the dissociation pathway of ketene along the C−C bond elongation.

The reaction enthalpies and free energies of oxygen abstraction reactions by C atom obtained in this study are summarized in Table 5. Our results are in very good agreement with experimental results. The reaction C + CH_2O → CO + CH_2 is highly exoergic, and the reaction free energy of the excited singlet $^1B_1$ carbene producing the reaction is calculated to be −75.1 kcal/mol (Table 5).

Table 5. Reaction Enthalpies at 0 K (ΔH_0) and 298 K (ΔH_{298}) and Free Energies at 298 K (ΔG_{298}) at the MCPT Level (in kcal/mol)

		ΔH_0	ΔH_{298}		ΔG_{298}
reactants	products	calc	calc	exp[a]	calc
C (^{3}P) + CH_2O	**T2** ($^3A''$)	−97.7	−98.7	−101.2[b]	−91.1
C (^{1}D) + CH_2O	**S2** ($^1A_1$)	−179.0	−180.1	−184.1	−171.7
T2 ($^3A''$)	CO + CH_2 ($^3B_1$)	20.7	22.3	24.5[b]	12.9
S2 ($^1A_1$)	CO + CH_2 ($^1A_1$)	84.9	86.6	87.3	76.2
S2 ($^1A_1$)	CO + CH_2 ($^1B_1$)	105.4	107.1	112.2	97.0
S2 ($^1A_1$)	CO + CH_2 (c^1A_1)	128.0	130.5	138.4	123.1
C (^{3}P) + CH_2O	CO + CH_2 ($^3B_1$)	−77.0	−76.4	−76.7	−78.2
C (^{1}D) + CH_2O	CO + CH_2 ($^1A_1$)	−94.1	−93.5	−96.8	−95.5
C (^{1}D) + CH_2O	CO + CH_2 ($^1B_1$)	−73.6	−73.0	−72.9	−75.1
C (^{1}D) + CH_2O	CO + CH_2 (c^1A_1)	−51.1	−49.6	−45.7	−48.6

[a] ΔH_{298} values are given. For detailed information about the experimental values, see Table 2. [b] **T2** energies are calculated from a **S2** ($^1A_1$)−**T2** ($^3A''$) separation of 54.8 kcal/mol, reported by Schaefer in ref 18b, with heat capacity corrections obtained in this study.

After a thorough examination of the C + CH_2O PES, we feel that singlet excited carbene generation is not a likely

(41) (a) Carpenter, B. K. *Angew. Chem., Int. Ed.* **1998**, *37*, 3340. (b) Carpenter, B. K. In *Reactive Intermediate Chemistry*; Moss, R. A., Platz, M. S., Jones, M., Jr., Eds.; Wiley-Interscience: New York, 2004; p 925. (c) Carpenter, B. K. *Annu. Rev. Phys. Chem.* **2005**, *56*, 57.

(42) (a) Sustmann, R.; Ansmann, A.; Vahrenholt, F. *J. Am. Chem. Soc.* **1972**, *94*, 8099. (b) Bernardi, F.; Bottoni, A.; Olivucci, M.; Robb, M. A.; Schlegel, H. B.; Tonachini, G. *J. Am. Chem. Soc.* **1988**, *110*, 5993. (c) Houk, K. N. *Pure Appl. Chem.* **1989**, *61*, 643. (d) Woodward, R. B.; Hoffmann, R. *Angew. Chem., Int. Ed. Engl.* **1969**, *8*, 781. (e) Staudinger, H. *Die Ketene*; Enke: Stuttgart, 1912. (f) Rey, M.; Roberts, S.; Dieffenbacher, A.; Dreiding, A. S. *Helv. Chim. Acta* **1970**, *53*, 417. (g) Brady, W. T.; Roe, R., Jr. *J. Am. Chem. Soc.* **1971**, *93*, 1662. (h) Brook, P. R.; Harrison, J. M.; Duke, A. J. *Chem. Commun.* **1970**, 589.

Table 6. Relative Energies (kcal/mol), Enthalpies (kcal/mol) at 0 and 298 K, and Free Energies (kcal/mol) at the PBE1PBE/6-311+G(2d,p) Level of Species on the Ketene Plus (*Z*)-2-Butene Potential Energy Surface

	ΔE	ΔH_0	ΔH_{298K}	ΔG_{298K}
cis-butene + ketene	0.0	0.0	0.0	0.0
TS1	38.4	40.2	39.2	51.3
cis 5ring	14.7	19.9	18.1	32.0
TS2[a]	51.9	50.6	50.7	59.5
cis-cyclopropane + CO	−9.6	−7.6	−8.0	−6.2
TS3[a]	36.5	37.4	36.8	47.4
cis biradical[a]	27.6	29.7	29.1	39.9
TS4	31.3	33.8	32.5	45.0
trans biradical[a]	26.5	28.5	28.0	38.7
TS5[a]	30.8	33.1	31.8	44.4
trans 5ring	13.5	18.5	16.8	30.4
TS6[a]	51.2	49.8	49.8	59.4
trans-cyclopropane + CO	−10.9	−9.0	−9.4	−7.1
TS7	24.3	26.8	25.5	38.4
cyclobutanone	−28.2	−23.2	−24.7	−11.5
TS8[a]	31.1	32.8	31.8	43.4
biradical[a]	29.7	31.7	31.1	41.7
TS9[a]	51.0	49.5	49.6	58.1

[a] Spin broken-symmetry solutions.

explanation for the experimental observation reported by Shevlin and co-workers.[13] Hence, we explored the possibility that (*Z*)-2-butene could trap "hot" ketene. Ketene is known to react with π-bond systems.[42] Therefore, it is possible that the ketene formed from the reaction of C (^{1}D) atom with formaldehyde can add to (*Z*)-2-butene and then undergo several steps of rearrangement to give the observed products, CO and cyclopropane. The reaction between ketene and (*Z*)-2-butene was studied by using the same PBE1PBE density functional with a 6-311+G(2d,p) basis set. Relative energies, enthalpies, and free energies are reported in Table 6, and a schematic potential energy surface for the reaction of ketene and (*Z*)-2-butene is given in Figure 7. Ketene can react with (*Z*)-2-butene in three ways: [2+3] concerted addition to a π-bond, C−C coupling addition followed by rotation around the C−C bond, and [2+2] cycloaddition. The [2+3] concerted addition has the highest enthalpy barrier (39.2 kcal/mol), and C−C coupling addition is second highest (36.8 kcal/mol). The lowest pathway is the well-known [2+2] cycloaddition[42] (25.5 kcal/mol), which will lead to a stable cyclobutanone. The C−C coupling addition will lead to a cis biradical intermediate, which can isomerize to a trans biradical intermediate. Both biradical intermediates can undergo ring closure to yield cyclopropane and CO as products. More likely, ketene will follow the lowest enthalpy pathway to form cyclobutanone, which can undergo ring-opening to a biradical followed by release of CO to form *trans*-1,2-dimethylcyclopropane. In "room temperature" chemical reactions, cyclobutanone can be isolated. However, because ketene is formed from the reaction of C (^{1}D) atom with CH_2O, 170 kcal/mol extra energy is carried over. Thus, the new-born cyclobutanone is formed very hot, and the C−C bond can be broken easily. The three pathways to the products are very competitive, since their enthalpic barrier heights are similar (50.7, 49.8, and 49.6 kcal/mol). If the ketene encounters (*Z*)-2-butene before relaxation, these high barriers can be overcome easily. Therefore, we suggest that this is the best explanation for the observed *cis*-

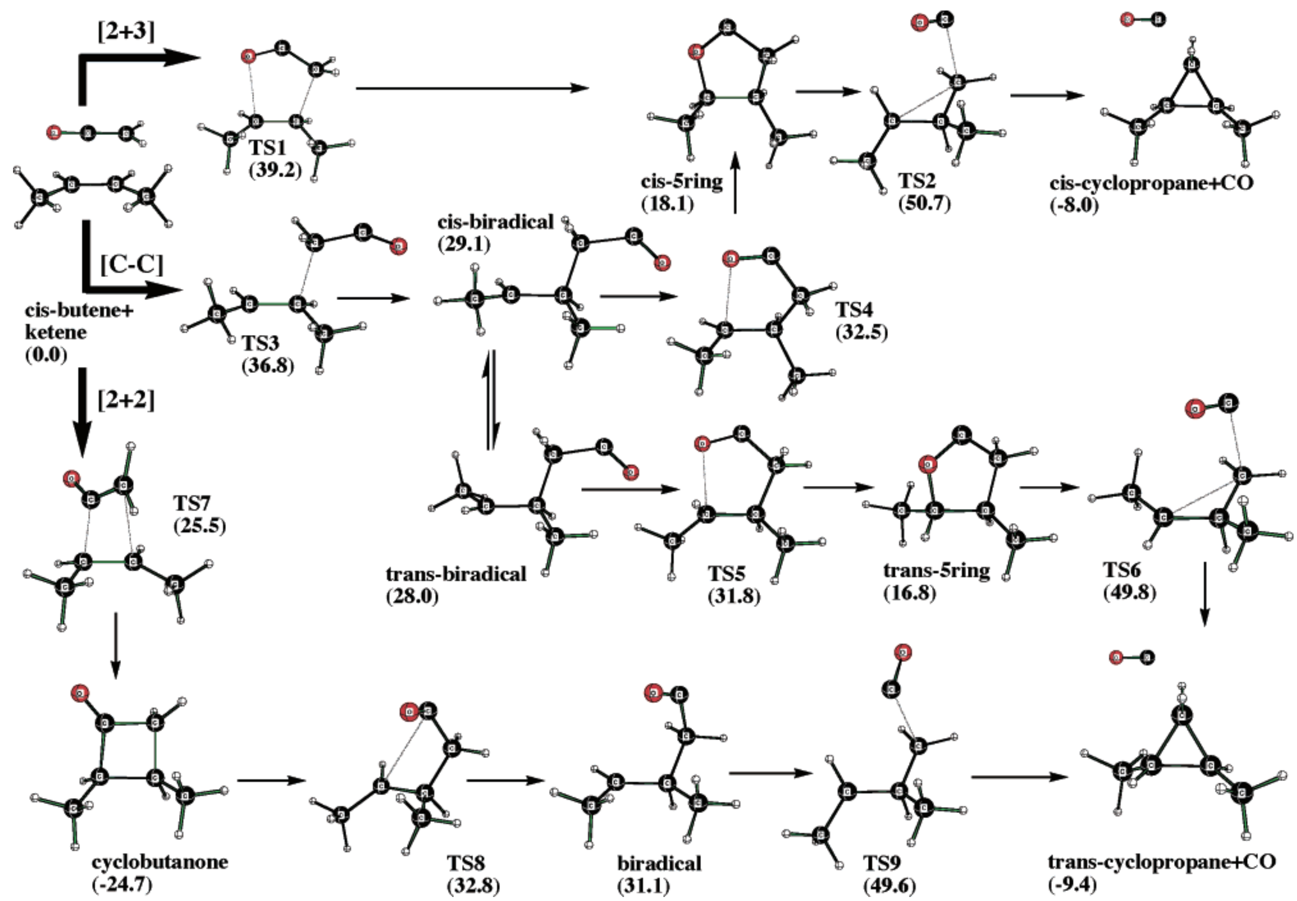

Figure 7. Potential energy surface for the reaction of ketene with (*Z*)-2-butene. The values in parentheses are enthalpies at 298 K in kilocalories per mole calculated at the PBE1PBE/6-311+G(2d,p) level.

and *trans*-1,2-dimethylcyclopropane formation in the C atom reaction with formaldehyde. We find it interesting that 25 years ago Dewar and co-workers proposed[10] a similar mechanism of carbene formation via a ketene intermediate in the reaction of C atoms plus butanal.

Conclusion

The reactions of triplet (^{3}P) and singlet (^{1}D) atomic carbon with formaldehyde were studied computationally. Ketene **S2** ($^1A_1$) is the global minimum on the CH_2CO potential energy surface. On the triplet PES, a C atom adds to the C−O double bond to form cyclic **T1**, which undergoes intramolecular rearrangement. The bent $H_2C{-}C{-}O$ linkage ketene isomer (**T2**) is lowest on the triplet PES, and it dissociates to give CO and the ground-state methylene ($^3B_1$). On the triplet surface, linear C−C−O or C−O−C isomers (**T22′** and **T55**) were found to be transition states for the interconversion of corresponding bent isomers (**T2** and **T5**). Hydrogen abstraction from formaldehyde by C (^{3}P) is nonspontaneous (4.1 kcal/mol) and can proceed without a reverse free energy barrier. On the singlet surface, the C (^{1}D) addition to the C−O double bond also occurs without barrier to form **S1** with a free energy change of −103.0 kcal/mol. Intermediate **S1** can also undergo various isomerization reactions to form the global minimum **S2** or **S5**, which is the second lowest species on both potential energy surfaces. On both surfaces, intermediate carbenes are identified (**T4** and **S3**).

Two possible pathways to form excited singlet methylene ($^1B_1$) were found. One is along the reaction path **Sr7**($^1A_2$) → **S7**($^1A''$) → **S7p**($^1A''$), which leads to the $^1B_1$ carbene directly, and the other is by way of **S2″**, which is the lowest-erergy species on the $^1A''$ surface. Interestingly, the ground state **S2** ($^1A_1$) correlates with the third excited singlet state methylene (c^1A_1) rather than the first excited singlet methylene ($^1A_1$). We also suggest that an alternative explanation of formation of *cis*- and *trans*-1,2-dimethylcyclopropane by the reaction of energetic ketene with (*Z*)-2-butene. The ultimate answer to products of the C + $CH_2{=}O$ reaction requires a consideration of the dynamic behavior. We are currently carrying out ab initio molecular dynamics calculations on the basis of our constructed potential energy surfaces.

Acknowledgment. Computer time was made available on the Auburn COSAM PRISM cluster and the Alabama Supercomputer center SGI Altix cluster.

Supporting Information Available: Table S1, Cartesian coordinates of all optimized structures obtained at the CASSCF-(14,13)/6-311+G(2d,p) level in Table 1; Table S2, the absolute energies (hartrees), zero-point energies (kcal/mol), heat capacity corrections to 298 K (kcal/mol), entropies (cal/mol·K), and spin-squared values at the PBE1PBE/6-311+G(2d,p) level for the species in Table 6; the full citation to ref 24 is given. This material is available free of charge via the Internet at http://pubs.acs.org.

JA060216M